Cooperative Cellular UAV-to-Everything (C-U2X) communication based on 5G sidelink for UAV swarms

Cooperative Cellular UAV-to-Everything (C-U2X) Communication based on 5G Sidelink for UAV Swarms

Debashisha Mishra[a,*], Angelo Trotta[b], Emiliano Traversi[c], Marco Di Felice[b] and Enrico Natalizio[a,d]

[a]*Université de Lorraine, CNRS, LORIA, France*
[b]*Department of Computer Science and Engineering, University of Bologna, Italy*
[c]*LIPN, UMR CNRS 7030, Université Sorbonne Paris Nord, France*
[d]*Technology Innovation Institute, United Arab Emirates*

ARTICLE INFO

Keywords:
UAV swarm
3GPP Sidelink
Cellular UAV-to-Everything (C-U2X)
Channel Scheduling
Multi-hop
Consensus-Based Bundle Algorithm (CBBA)

ABSTRACT

A swarm of cellular-connected Unmanned Aerial Vehicles (UAVs) enables new possibilities for emerging services and applications as the UAVs can autonomously coordinate their activities and cooperate to accomplish a given task. Because of spatio-temporal dynamics of swarm topology, robust and reliable network formation with seamless connectivity among UAVs is highly critical for any successful mission. This work focuses on the problem of cooperative and communication-aware UAV channel scheduling of data transmission from a set of target points of interests (PoIs) towards a cellular base station (BS). A novel, cooperative multi-hop communication model based on the C-V2X (Cellular Vehicle-to-Everything) Mode 4 cellular sidelink (PC5) radio interface is presented for efficient UAV data flow scheduling within the swarm. The model design aims at optimizing the cellular communications on UAV-to-UAV (U2U) and UAV-to-Infrastructure (U2I) links via a novel interference-aware scheduling, hence envisioning a new Cellular UAV-to-Everything (C-U2X) communication paradigm. An optimization model is used to solve the centralized version of the problem, while a distributed Dynamic Consensus-Based Bundle Algorithm (D-CBBA) is proposed to generate the best subchannel scheduling for maximizing data transmission in a distributed setting. Extensive simulation results demonstrate that the proposed distributed algorithm is able to extend the cellular infrastructure coverage while improving the multi-hop communications by autonomously adapting to the network conditions.

1. Introduction

The competitive advantages brought by Unmanned Aerial Vehicle (UAV) cellular communications, powered by mutual synergies of both cellular industry and UAV technology, is long agreed in the literature and investigated for different scopes [1][2]. Indeed, from the one the side, UAV-assisted cellular communication systems aim to employ UAVs as flying (or aerial) base stations or as relays to enhance existing terrestrial cellular communication or to mitigate disaster situations. On the other side, in cellular-assisted UAV communication scenarios, the UAV is integrated into the cellular network infrastructure as a new aerial user (flying UE) to support multitudes of diverse applications and use cases pertaining to industrial IoT [3], sensing, parcel delivery, infrastructure monitoring, just to name a few. The latter paradigm is also commonly referred as cellular-connected UAV [4, 5], and introduces several advantages in terms of operational range, Quality of Service (QoS) support and security compared to traditional solutions where the UAV transmits on the unlicensed frequency spectrum (e.g., LoRa, Wi-Fi, Zigbee etc).

In this paper, we consider a scenario where a group of cellular-connected UAVs must collaborate as a swarm in order to monitor a target region and to stream back the sensing data to a remote Base Station (BS). The collaborative multi-UAV deployment allows the devices to self-organize without or with little manual intervention, while increasing the area covered by the service [6]. Moreover, the usage of a swarm of cellular-connected UAVs can be far more economical as compared to a single cellular-connected UAV pursuing a mission [7, 8]. However, those benefits are realized with increased complexity and additional design challenges which must take into account the spatio-temporal dynamics of the aerial topology [9] as well as the characteristics of network architectures enabling cellular-connected UAV swarms. The latter can be subdivided in the two broad classes shown in Fig. 1, respectively:

- *Centralized Architecture* (Fig. 1a): in this approach, the cellular base station (BS) acts as a command center for guiding and controlling the fleet of UAVs. Each UAV transmits the surveillance and monitoring information to the BS via UAV-to-Infrastructure (U2I) links. There are no direct point-to-point links between two UAVs within the swarm. Massive MIMO, a vital technology component of emerging 5G standards, has been demonstrated to be a viable solution for supporting centralized swarm model of cellular-connected UAVs coexisting with cellular ground UEs [10, 11].
- *Decentralized Architecture* (Fig. 1b): in this approach, not all the UAVs are connected to the BS for control and communication. In addition to the U2I links, a UAV can communicate directly with another

E-mails: debashisha.mishra@univ-lorraine.fr (Debashisha Mishra), angelo.trotta5@unibo.it (Angelo Trotta), emiliano.traversi@tii.uae (Emiliano Traversi), marco.difelice3@unibo.it (Marco Di Felice), enrico.natalizio@tii.ae (Enrico Natalizio)
*Corresponding author.

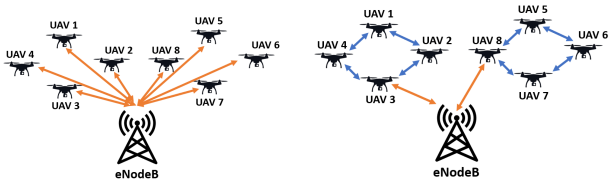

(a) Centralized Model (b) Decentralized Model

Figure 1: Cellular-connected UAV swarm architectures

peer UAV within the swarm to exchange information through UAV-to-UAV (U2U) communication links. The latter are enabled by the sidelink technology which has been proposed by the 3GPP consortium since release-12 as D2D Proximity Service (ProSe) feature to support public safety networks.

Many recent studies investigated the possibility to setup cellular D2D communication systems in both static and vehicular environments, e.g. by addressing the issue of device discovery, resource allocation and interference mitigation with the BSs [12, 13]. In addition, all releases of 3GPP after release-12 included standardization items for Vehicle-to-Everything(V2X) scenarios. However, the application of sidelink for U2U communications in swarm of cellular-connected UAVs has been barely addressed so far, also due to the additional complications posed by the aerial environments. Indeed, the interference effects experienced by the airborne UAVs are considerably different from the ground UEs, since they may fly much above the BS antenna height. Also, the 3D mobility can impact the cellular coverage in a significant way. Finally, the mission-oriented nature of the UAV swarm can be exploited to allocate channel resources by taking into account the current positions and the future trajectories of the aerial devices.

In this paper, we address the aforementioned research issues by investigating the deployment of swarms of cellular-connected UAVs based on Cellular-U2X (Cellular UAV-to-Everything) communication. To this purpose, we focus on the decentralized architecture of Fig. 1b, including both U2U and U2I links, and we provide fundamental results on channel allocation and scheduling issues. More in details, three main contributions are described in this paper:

- We discuss the main issues of 3GPP sidelink technology for inter-UAVs communications and provide a comprehensive characterization of C-U2X links in terms of coverage probability for the U2I and U2U links. Through numerical results, we compute the average link quality improvement when the UAV swarm uses U2U links, hence justifying the usage of sidelink technology for aerial communications.
- We introduce a new optimization problem, called Multi-Channel Flow Optimization Problem (MCFOP) that computes the optimal data flow scheduling for a swarm of cellular-connected UAVs in a centralized way. We prove that the problem itself is NP-hard, and for this reason we introduce an optimization model where the objective function consists of a linear and a quadratic part. The proposed model is able to optimize simultaneously both the routing of the information and the allocation of different sub-channels.
- We extend the study to the distributed scenario without any central authority (in our case, the BS) and propose two distributed algorithms for channel allocation and transmission scheduling. Specifically, we describe an extension of the popular auction-based Consensus-Based Bundle Algorithm (CBBA) to produce a conflict-free assignment of transmission opportunities to the UAVs.

The performance analysis demonstrates that our Dynamic CBBA (D-CBBA) algorithm is able to face the dynamicity of multi-hop UAV networks by executing almost 80% of the data transmissions without causing harmful interference in the multi-hop network. Moreover, D-CBBA greatly overcomes the basic CBBA and the greedy schemes, while it approaches the optimal results produced by the centralized MCFOP solution.

The rest of the paper is organized as follows: Section 2 reviews the existing literature on the sidelink communication and its use on multi-hop UAVs networks. Section 3 provides characterization of sidelink for U2U/U2I communication and evaluates its performance. The system model along with scenario description and problem formulation is discussed in Section 4. The description of centralized and distributed algorithms is presented in Section 5. Experimental performance analysis of the proposed algorithms is given in Section 6. We conclude the paper and discuss future works in Section 7.

2. Related Works

We split the literature review into three Sections that discuss different aspects of our work. In Section 2.1 we provide a brief overview of sidelink technologies and standardization efforts from the 3GPP. In Section 2.2 we review the state of the art concerning cellular-connected UAVs and UAV-to-X communications. Finally, in Section 2.3 we discuss channel scheduling algorithms. Given the lack of studies focusing on our specific research problem (i.e. scheduling in cellular UAV swarms), we broaden the review to other multi-hop wireless networks.

2.1. Overview of Sidelink technology and 3GPP Standardization Efforts

Sidelink defines a competent cellular technology which enables direct transmission between devices with or without involvement of cellular BSs. This technology is investigated by 3GPP starting from release-12 as D2D Proximity Service (ProSe) feature to support public safety networks. More specifically, dedicated physical layer channels

such as Physical Sidelink Shared Channel (PSSCH), Physical Sidelink Control Channel (PSCCH), Physical Sidelink Broadcast Channel (PSBCH), Sidelink Control Information (SCI) have been created with the specific purpose to support sidelink transmission, synchronization and device discovery. Each sidelink channel is split into a time-frequency resource grid structure: in time domain, 1 *ms* subframes and in the frequency domain, a set of contiguous resource blocks (RBs). A subchannel defines a group of RBs in the same subframe. The number of RBs in subchannel can vary depending upon the configuration. Both sidelink mode 1 and 2 share the same resource structure where direct communication is performed by scheduling the time-frequency resources from the resource pool that comprises of repeating sequence of hyperframes called Scheduling Assignment (SA) or PSCCH period. Each SA period owns resources for control (carried via PSCCH) and data (carried via PSSCH). PSCCH carries the SCI (Sidelink Channel Information) containing details about the modulation and coding scheme, the RBs used, resource reservation interval.

A Transport Block (TB) contains a full packet to be transmitted via PSSCH. In mode 3 and 4, the SA is transmitted using specific RBs in subchannel and TB transmission can occupy the adjacent or non-adjacent RBs in the same subframe. Figure 2 shows both type of resource pool structure. Sometimes, more than one device may occasionally select the same resources from the shared pool leading to resource conflict. Hence, such selections are coordinated using proper collision resolution methods. The current scheduling algorithm is a sensing-based semi-persistent scheduling [14] where each node can choose the time-frequency resources to use. The algorithm does not provide any coordination among the competing nodes; the nodes have to apply a sensing-based mechanism to identify the least used time-frequency resources.

Sidelink has already been shown to be useful in Vehicle-to-Everything (V2X) and maritime communication [15, 16]. Release-14 of 3GPP included many additional standardization items for V2X that encompasses Vehicle-to-vehicle (V2V), Vehicle-to-infrastructure (V2I), Vehicle-to-Network (V2N). 3GPP release-15 and release-16 include further safety related enhancements to V2X communication (eV2X) like automated and remote driving, platooning of vehicles [17, 18].

Among others, two main components of sidelink technology have been extensively revised by standardization bodies and investigated by the research community, *i.e.,* the (a) device discovery and the (b) resource allocation. The discovery corresponds to the ability to locate another device, which is in proximity, by using sidelink (PC5) radio interface, and it can be done directly by the UE or at the core network level. The notion of proximity can be extended to the quality of radio channel experienced between communicating UE pairs, signal quality, delay, throughput, network load, etc. Regarding the resource allocation, two sidelink resource allocation modes for public safety [15] are available in 3GPP release-12, respectively *i.e.,* mode 1 (scheduling performed by eNodeB) and mode 2 (devices autonomously manage the resource scheduling). Mode 1 and 2 are primarily used for prolonged battery life at cost of higher latency. In release-14, standardization of C-V2X introduced two additional resource allocation modes [16] designed to cater reliable and latency sensitive communication *i.e.,* mode 3 (in which scheduling is managed by network) and mode 4 (out-of-coverage vehicles autonomously select the resources using a distributed sensing-based semi-persistent scheduling (SPS) scheme).

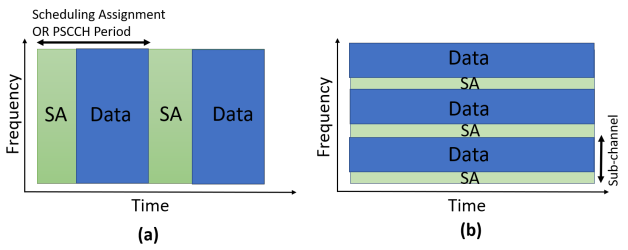

Figure 2: Resource Pool Structure: Mode (a) 1,2 (b) 3,4

The work in [19] highlighted the use of sidelink as one of the key candidate technology for enabling U2U communication in 5G and beyond (6G) networks. Authors in [20] analyzed the sidelink resource allocation for mode 1 C-V2X where the BS is in charge of scheduling the resources for the D2D communication. However, mode 1 and 3 envisage the continuous transmission of channel state information (CSI) to the BS. Due to the dynamic nature of UAV wireless networks, this mode is infeasible for multi-hop communication. On the contrary, mode 2 and 4 enable the autonomous selection of the resources for data transmissions over sidelink channels. Mode 4 uses as resource scheduling the Semi-Persistent Scheduling with Listen-Before-Talk (LBT) strategy. However, this method is found to be unable to cope with high network load [16]. To this aim, the authors in [21] showed that a congestion control mechanism can mitigate the channel degradation.

2.2. Cellular UAV-to-X communication

The realization of a swarm of cellular-connected UAVs has not been demonstrated so far experimentally and related literature, in this regard, is unavailable. Even though it is foreseen and inclusion of U2U communications in the next 3GPP releases to support new UAVs applications is gaining high attention [22], very few works have considered the U2U communication being supported by the cellular spectrum. A preliminary study was introduced in [23] to motivate the use of sidelink for establishing efficient intra-swarm U2U communication for extending the connectivity for out-of-coverage UAVs during mission. Moreover, the majority of the works considers single-hop communications only. For what concerns the use of sidelink, in [24], the authors investigated U2U communication in a scenario where the UAV pairs share a portion of uplink spectrum resources of ground users in an underlay manner. The study aims at improving

Table 1
Summary of similar works and contributions

Reference Work(s)	Focus of the study	Contributions/Solutions
[16]	LTE V2X Sidelink	An overview of LTE-V standard for sidelink V2V communication, Comparison of LTE-V with other short-range solutions like 802.11p or DSRC. Proposed a modified sensing-based semi-persistent scheduling for efficient channel resource selection.
[15]	LTE V2X Sidelink	Adances of D2D sidelink for enhanced V2X communication. Performance anlaysis semi-persistent scheduling for D2D modes 3 and 4 via system-level simulations.
[17]	3GPP NR V2X Sidelink	Performance evaluation to assess the gains of the new control channel design of 5G NR.
[18]	Cellular V2X Sidelink	A comprehensive overview of 3GPP Release 16 NR SL design for NR V2X, the network architecture, security, and protocol enhancement.
[24], [25]	Cellular U2U	Performance analysis of U2U communication underlaying cellular uplink resources of ground UEs, Single-hop transmission path, Stochastic geometry based analysis.
[27]	Traditional Cellular Network	Multi-hop, multi-channel joint resource scheduling and routing formulated as MINLP problem to enhance network throughput.
[28]	Traditional Cellular Network	Multi-hop, sub-channel scheduling exploiting the frequency sharing among hops to achieve higher spectral efficiency, Mathematical modeling and optimization.
This work	*Cellular U2X Sidelink*	*Characterization of U2U sidelink and multi-hop resource (sub-channel) scheduling among UAVs for data transmission in a cellular-connected UAV swarm, Performance evaluation and complexity analysis of both centralized and distributed algorithm implementation. .*

the link performance of both U2U and uplink by adopting tools from stochastic geometry.

The same authors extended the analysis in [25] where UAV pairs share the same spectrum in uplink with ground users considering both underlay and overlay spectrum sharing settings. Note that, above two reference works split the spectrum resources allocated to uplink of cellular ground users, thereby requiring additional interference handling mechanisms. In underlay setting, same spectrum serves both U2U and cellular uplink transmission, hence it is prone to mutual interference from other U2U and ground user uplink transmission. In overlay, the achievable rate is compromised, because the spectrum resources are dedicated separately (non-overlapping) for U2U and cellular uplink. In [26], the authors propose to optimize the cellular UAV-to-X communications: with given routing information, the uplink sum-rate is maximized, while the quality of the sidelink communication is handled by imposing a constraint on the minimum transmission rate for each sidelink.

2.3. Multi-hop multi-channel scheduling

Due to the multi-hop multi-channel nature of the communications inside the UAV swarm, channel scheduling algorithm must be designed in order to optimize the wireless resources used during the U2U communications. Resource allocation in dense UEs scenarios has been studied in [29] in order to establish a set of device-to-device multi-hop multi-path (MHMP) communications in 5G networks. Here the authors studied the sharing of downlink channel for distributed video content delivery. The proposed optimization problem is derived from the definition of the channel quality and then the channel scheduling is modelled to ensure the maximum channel capacity in the communications. In [30], the authors defined a Non Linear Integer Programming (NLIP) model for channel assignment to minimize mutual interference in different wireless transmission links.

The works aforementioned do not take into consideration the time dimension of the problem and the actual transmissions on the wireless links. In a scenario of a multi-radio multi-channel multi-hop cognitive cellular network, the authors in [27] defined a joint scheduling and routing optimization problem using a mixed integer non-linear programming (MINLP), but the impact of interference was been taken into account. Similarly, the study in [28] presents a framework of frequency sharing in multi-hop OFDM networks for a chain topology.

However, none of the aforementioned works analyzed the scheduling problem in a multi-hop scenario for a cellular-connected UAVs network. In this work, we focus on the implementation of a distributed channel scheduler for Mode 4 over 5G sidelink communication that is able minimize the collision among the UAVs transmissions, focusing on the peculiarities of aerial communications, such as Line-of-Sight (LoS) transmission links and multi-hop communications. In Table 1, we highlight similar works found in the literature that align with different aspects of the contributions made in this work.

3. Preliminary Study on the C-U2X Sidelink

In this Section, we provide preliminary results about the application of sidelink. First, in Section 3.1, we discuss challenges and unique characteristics of aerial sidelink communications with respect to the well-investigated terrestrial scenarios. Then, in Section 3.2, we derive the probability of successful transmission for U2I and U2U links showing numerical results demonstrating the advantages of using U2U links for swarm formation.

3.1. Envisioning Sidelink for UAV-to-UAV (U2U)

D2D-enabled ProSe technology over PC5 interface is already revolutionizing the data transmissions for terrestrial Machine Type Communications (MTC) [15, 16]. Indeed, adaptation of terrestrial sidelink is primarily targeted for direct communication among ground UEs. In cellular UAV-swarms, nearby devices flying in proximity and joining the same mission can take advance of the sidelink feature to forward data towards the BS as well as to exchange control data among them. At the same time, aerial UAVs pose additional complications and novel opportunities for U2U communication which are briefly summarized as follows.

Dimensionality of Environment **-** Terrestrial UEs mostly operate in 2D area where the height of the receiver is typically a few meters. In addition, these devices move horizontally and are surrounded by the 2D coverage of cellular BS. Vice versa, UAVs are flying entities that operate in a 3D space with varying altitude, and the latter produces a non-negligible impact on the coverage criterion and the average U2U link quality.

Propagation Medium **-** UAVs are airborne devices staying at a much higher altitude than the terrestrial UEs or automotive vehicles. With increase in the height above ground, radio environment changes drastically. Usually UAVs fly much above the BS antenna height. Hence, the UAVs may experience dominant LoS probability from different ground BSs that contribute to high interference at the UAV receivers. Additionally, due to the relative velocity of UAVs during mission, there exists a space-time correlation effect on the U2U link.

Path Planning Optimization **-**. The UAVs mostly plan their path and optimize the trajectory in a 3D space depending on the mission objective and on coverage/connectivity constraints. Vice versa, terrestrial UEs do not consider path planning as an optimization objective because their movements are often not tied to any real-time mission, or because the overall trajectories are known by the users/drivers but not by the devices. The path awareness may constitute an advantage for the sidelink deployment, since the scheduling of data transmissions on U2U links may take into account the current and future positions of the UAVs and hence the evolution of the wireless links.

Energy Constraints **-** Energy saving constitutes already an issue for battery powered terrestrial UEs. However, it becomes a vital bottleneck in case of aerial UAVs where the flight autonomy is extremely limited. As a result, network-intensive sidelink mechanisms e.g. related to device discovery or computationally-intensive resource allocation strategies must be carefully evaluated for the case of cellular UAV swarms.

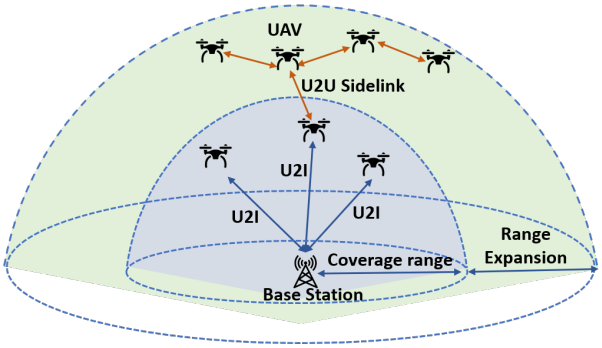

Figure 3: System Diagram

3.2. Communication Link Characterization

In the following, we study and analyze both U2I and U2U communication links taking into consideration the shared nature of the sidelink mode 4 channels. The U2I links leverage cellular (Uu) radio interface to connect UAVs to the BS for high payload services in uplink and essential CNPC in downlink. The U2U links are used to disseminate periodical safety critical and payload information via sidelink (PC5) radio interface with D2D ProSe communication. These links provide support to robust and reliable communication for multiple UAVs in fully-connected manner.

We investigate the coverage performance of sidelink (U2U) compared with the cellular infrastructure (U2I) links for considering an architecture depicted in Fig. 3. For modeling the UAVs and the BSs for the network deployment in a swarm of cellular-connected UAVs, tools from stochastic geometry, spatial statistics and point processes are used. These tools not only result in tractable approach for estimating rate and coverage of the deployment, but also assist in deriving important insights concerning the adopted model. We consider a multiple deployment realization in which each realization consists of an evaluation environment with multiple

Table 2
Glossary of Environmental Parameters

Parameter	Value
Reference Pathloss	$28 + 20 \cdot log10(f_c$ in GHz)
Pathloss exponent (LoS)	2.2
Pathloss exponent (NLoS)	$4.6 - 0.7log10(H_u)$
Small scale fading	Nakagami-m fading model
LoS probability	ITU model, Eqn.4 of [31]
Height of UAV (H_u)	100 meters
BS Density per m^2 (λ_b)	0.01
UAV Density per m^2 (λ_u)	0.05
Noise Figure	7 dB
Thermal Noise	-104 dBm/Hz
Antenna Gain	Omnidirectional with 6 dB
UAV Transmit Power	24 dBm

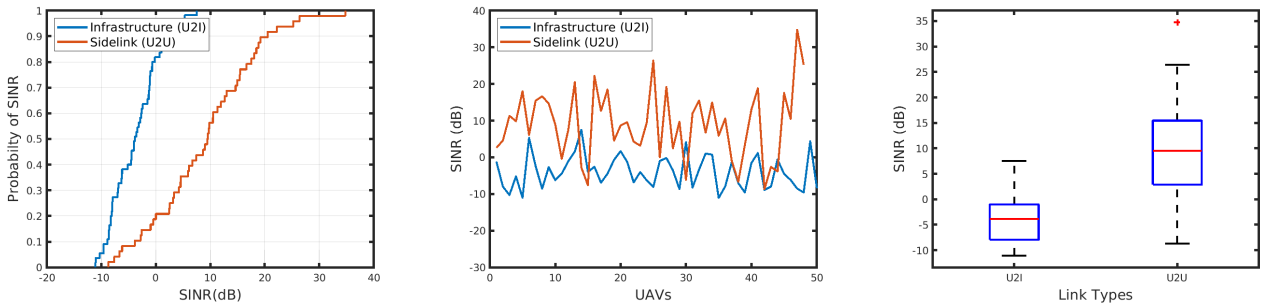

(a) CDF of SINR distribution (b) Instantaneous SINR distribution (c) Box plot showing SINR dispersion

Figure 4: Coverage comparison of sidelink (U2U) with infrastructure (U2I) links

terrestrial base stations and multiple UAVs being served by those base stations. We assume that the base stations are deployed by a single operator in 2D space and their locations are modeled as per Matern hard core point process type II (MHCPP-II) with density $\lambda_b = 0.01$ per square meters [32]. We model the UAV distribution as per Poisson Point Process (PPP) with altitude $H_u = 100$ meters and density $\lambda_u = 0.05$ per square meters. The UAVs are assumed to be positioned in 3D coordinate system and connected to their serving BS according to strongest received signal strength. For accuracy, both UAV-to-Ground and UAV-to-UAV channel includes large-scale fading along with small-scale fading and shadowing. Table 2 summarizes the essential parameters about the propagation environment used in the experiment.

In Fig. 4, we demonstrate SINR distribution for U2U and U2I links. As shown in Fig. 4a, U2U link performance is improved as compared with U2I links. Considering 0 dB as a baseline for SINR comparison, nearly 80% of UAVs experience good SINR coverage (more than 0 dB) for U2U links whereas 20% of UAVs experience good SINR more than 0 dB for U2I links. Hence, sidelink (PC5) radio interface can improve the link throughput to support data transmission services. In Fig. 4b, we show the variation of instantaneous UAV SINR values for both U2U and U2I links. Overall range of SINR dispersion for both type of links with five number summary (minimum, first quartile, median, third quartile, and maximum) is presented in the box plot shown in Fig 4c. It is evident that UAVs are provided with good coverage by the U2U links as compared to the U2I links.

4. System Modeling and Problem Formulation

4.1. Scenario Description

We consider a generic video monitoring mission depicted in Figure 5, in which a swarm of cellular-connected UAVs must monitor a target region and stream back the sensing data to the BS. To this aim, we assume that the entire region is divided into small zones or Points of Interests (PoIs), marked as stars in the Figure. The PoIs are assumed to be static and their positions are known to the UAVs before mission execution. The UAVs have to hover over the PoIs and to transmit the video streams in real-time towards the BS, by using a combination of U2I and U2U links. The focus of this paper is on the cellular communication issues; hence, we abstract from details of the specific application in use, by the meaning of the PoIs and by the multimedia aspects. However, it is worth remarking that the target scenario can fit the characteristics of several applications of UAV swarms, i.e. related to environmental or crowd monitoring. To meet the mission's objectives, UAVs must fly around the target PoIs, possibly beyond the supported communication range from the BS, thus incurring in potential disconnections and reducing the overall throughput of the monitoring system. This case is shown in Figure 5b and corresponds to a random and non-cooperative deployment of the UAVs where swarm connectivity constraints are not taken into account. On the opposite, Figure 5c depicts a fully cooperative deployment where some UAVs serve as relays (*i.e.,* UE relays) to extend the cellular coverage, hence ensuring a fully-connected swarm deployment.

Broadly speaking, the optimal deployment of a swarm of cellular-connected UAVs for monitoring mission requires to simultaneously address two research issues:

- *Positioning*, *i.e.,* how to place the UAVs so that the maximum number of PoIs is covered while ensuring that each UAV is always connected to the BS via direct or multi-hop links;
- *Scheduling*, *i.e.,* how to allocate the data flows on the available radio time-frequency resources (*i.e.:* subchannels) so that the expected number of packets successfully received at the BS is maximized.

In this work, the two problems are addressed sequentially. First, the positions of the UAVs are computed by the BS. Then, the scheduling algorithms are executed. We rely on state-of-art solutions (see details in Section 5) for the positioning problem since this is not the main focus of the paper; interested readers can refer to our previous study [33] related to UAV swarm coverage and connectivity using centralized and distributed approaches. In the following, we formally model the scenario and introduce the objective function of the scheduling problem.

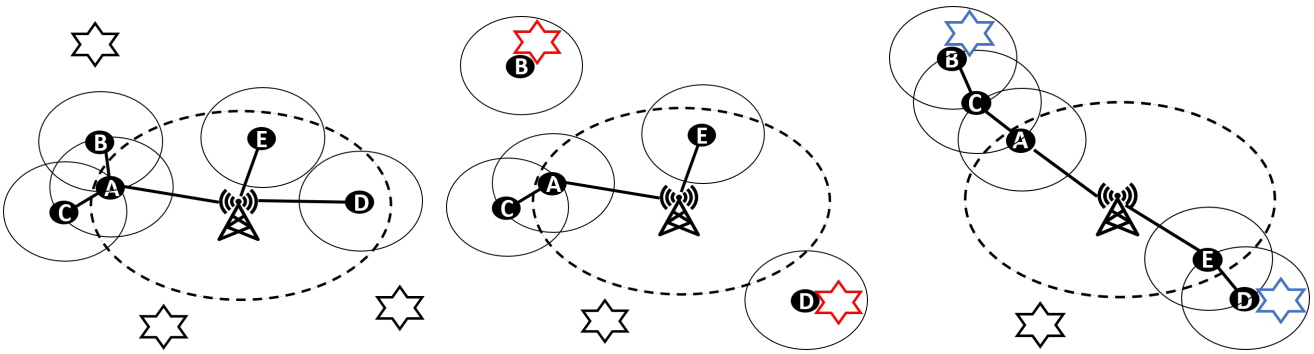

(a) Initial scenario (b) Non-cooperative planning (c) Spatio-temporal cooperative planning

Figure 5: Dynamic aerial network formation and coverage constraints

4.2. Scenario Modeling

Let $\mathcal{U} \triangleq \{u_1, u_2, \dots, u_{N_U}\}$ be a swarm of N_U cellular-connected UAVs in a 3D Cartesian coordinate system. Without loss of generality, we denote as D_{comm} the maximum range (as distance) for U2U communications. Similarly, with indicate with R_{comm} the maximum range for U2I communications. The swarm topology is modeled as a *layout graph* $\bar{G} = (\bar{V}, \bar{E})$ representing the relative positions of the UAVs. The set $\bar{V}$ contains one node for each UAV and for the BS: $\bar{V} = \{\langle u_1 \rangle, \dots, \left\langle u_{N_U} \right\rangle, \langle B \rangle\}$. The set $\bar{E} = \bar{E}_{UAV} \cup \bar{E}_B$ contains the U2U links and U2I links enabled by the communication ranges. More specifically, we indicate with $e = \{\langle u_i \rangle, \left\langle u_j \right\rangle\} \subseteq \bar{E}_{UAV} \subseteq \bar{V} \times \bar{V}$ the U2U link between UAVs $\langle u_i \rangle$ *and* $\left\langle u_j \right\rangle$, placed at distance lower or equal than D_{comm}. Similarly, we indicate with $e = \{\langle u_i \rangle, \langle B \rangle\} \subseteq \bar{E}_B \subseteq \bar{V} \times \langle B \rangle$ the link between UAV $\langle u_i \rangle$ and the BS, when their distance is lower or equal than R_{comm}. Each edge $e \in \bar{E}$ is associated to an integer transit time τ_e, corresponding to the delay (in terms of number of time slots) required to transmit a data packet over link e. The graph is assumed to be connected when the mission starts. The mathematical notations used to define our system model are summarized in Table 3.

In the following, we model the characteristics of the data sources and traffic load. We assume a finite number of subchannels $\mathcal{R} \triangleq \{r_0, r_1, r_2, r_3, \dots, r_{N_{\text{subc}}}\}$ (where r_0 is the buffering channel). Also, we assume a slotted time model, with a *finite* time horizon $\mathcal{T}$, divided into N_T time slots of equal length t_{slot}: $\mathcal{T} \triangleq \{t_1, t_2, \dots, t_{N_T}, t_{N_T+1}\}$. As described in Section 3, sidelink transmissions rely on a basic time subdivision with subframe of length 1 *ms*, hence $t_{\text{slot}} = 1$ *ms*. Let N_Z be the number of target PoIs. Let $\mathcal{U}_{z_j} \subseteq \mathcal{U}$ be the subset of UAVs that are involved in the data flow related to the target area z_j.

During the entire mission, we assume that N_{z_i} data packets are generated for PoI z_i, with a uniform data rate of N_g packets per second (constant over the PoIs). Let $\text{dt}_{z_i}^{t_w}$ be the data packet generated at time t_w for PoI z_i. We indicate with $\text{DT}_{z_i} \triangleq \{\text{dt}_{z_i}^{t_1}, \text{dt}_{z_i}^{t_2}, ..., \text{dt}_{z_i}^{t_{N_{z_i}}}\}$ the overall set of data packets generated at the target PoI z_i, and with $\text{DT} \triangleq \bigcup_{z_i \in \mathcal{Z}} \text{DT}_{z_i}$ the set of all the packets generated over the scenario during the entire mission. For ease of disposition, we use $\text{dt} \in DT$ to refer to a generic packet when there is no need to explicit the region and the time slot.

In order to model the scheduling of the data transmissions in the cellular UAV swarm, we introduce the concept of *multi-graph* $G = (V, A)$, a time-expanded directed version of the graph $\bar{G}$ that allows to model the transmissions of the data packets from the targets PoIs towards the BS during the time horizon considered. The set of vertexes $V = V_D \cup V_{UAV} \cup \langle B \rangle$ includes the following elements (in addition to B, the BS):

- $V_D = DT$ contains one vertex for each packet $\left\langle \text{dt}_{z_i}^{t_k} \right\rangle$ generated during the mission;
- V_{UAV} consists of tuples $\langle u_i, t_k \rangle$, $\forall u_i \in \mathcal{U}$, and $\forall t_k \in \mathcal{T}$. Item $\langle u_i, t_k \rangle$, $\forall u_i \in \mathcal{U}$ indicates that UAV u_i is using a subchannel in time slot t_k.

We indicate with $V(t_k) = \{v = \langle u_i, t_{k'} \rangle : k = k'\} \subseteq V$ the subset of vertices associated to time slot $t_{k'}$.
Similarly, the set of arcs $A = A_A \cup A_{BUF} \cup A_{TR} \cup A_B$ consists of the following elements:

- $A_A = \{\left(\left\langle \text{dt}_{z_i}^{t_k} \right\rangle, \langle u_i, t_k \rangle\right), \forall \text{dt}_{z_i}^{t_k} \in DT, \forall u_i \in \mathcal{U}_{z_j}, k = 0, \dots, N_T\}$ is the set of *assignment* arcs, associating the data packets produced by a PoI to a UAV that is covering that region;
- $A_{BUF} = \{\left(\langle u_i, t_k \rangle, \left\langle u_i, t_{k+1} \right\rangle\right)_{r_0, \text{dt}}, \forall r_j \in \mathcal{R}, u_i \in \mathcal{U}, \text{dt} \in DT, k = 0, \dots, N_T\}$ is the set of *buffering* arcs used to represent the possibility for a UAV u_i to delay the transmission of data packet dt at time t_k;
- $A_{TR} = \{\left(\langle u_i, t_k \rangle, \left\langle u_{i'}, t_{k+\tau_{ii'}} \right\rangle\right)_{r_j, \text{dt}}, \forall r_j \in \mathcal{R} \setminus \{r_0\}, \forall \{\langle u_i \rangle, \langle u_{i'} \rangle\} \in \bar{E}_{UAV}, \forall \text{dt} \in DT, k = 0, \dots, N_T\}$ is the set of *transmission* arcs used to represent the transmission of the data packet from u_i to $u_{i'}$ with subchannel r_j.
- $A_B = \{\left(\langle u_i, t_k \rangle, \langle B \rangle\right)_{r_j, \text{dt}}, \forall r_j \in \mathcal{R} \setminus \{r_0\}, \forall \{\langle u_i \rangle, \langle B \rangle\} \in \bar{E}_B, \forall \text{dt} \in DT, k =$

Table 3
Glossary

Notation	Definition
D_{comm}	Range of U2U communication
R_{comm}	Range of U2I communication
$\mathcal{U} \triangleq \{u_1, u_2, \dots, u_{N_U}\}$	Swarm of N_U cellular-connected UAVs
$\mathcal{Z} \triangleq \{z_1, z_2, \dots, z_{N_Z}\}$	Set of N_Z target point of interests (PoIs)
$\mathcal{T} \triangleq \{t_1, t_2, \dots, t_{N_T}, t_{N_T+1}\}$	Time horizon
N_{z_i}	Data packets generated for PoI z_i
$\mathcal{U}_{z_j} \subseteq \mathcal{U}$	The subset of UAVs involved in data flow related to target area z_j
$\mathcal{R} \triangleq \{r_0, r_1, r_2, r_3, \dots, r_{N_{\text{subc}}}\}$	Set of subchannels
r_0	Buffering channel
$\bar{G} = (\bar{V}, \bar{E})$	Layout graph of swarm
A_A	Set of *assignment* arcs
A_{BUF}	Set of *buffering* arcs
A_{TR}	Set of *transmission* arcs
A_B	Set of *base* arcs
$\text{rss}(a)$	The signal strength received at the destination UAV belonging to arc a
τ_e	Delay (number of time slots required to transmit a data packet) over link e
$\mathcal{W}_a$	The probability of successful transmission through arc a
N_0	Noise figure
φ_a	1 if arc $a \in A$ is selected, 0 otherwise
$\mathcal{U}_{z_j} \subseteq \mathcal{U}$	The subset of UAVs that are involved in the data flow
$\text{dt}_{z_i}^{t_w}$	The data packet generated at time t_w for PoI z_i
$\text{DT} \triangleq \bigcup_{z_i \in \mathcal{Z}} \text{DT}_{z_i}$	Set of all the packets generated over the scenario
$\delta^+(v)$, $\delta^-(v)$	The outgoing and incoming arcs of vertex v, respectively
$\delta^+_{r_j}(v)$, $\delta^-_{r_j}(v))$	The outgoing and incoming arcs using sub-channel r_j, respectively
$\delta^+_{\text{dt}}(v)$, $\delta^-_{\text{dt}}(v))$	The outgoing and incoming arcs related to data packet dt, respectively

$0, \dots, N_T + 1\}$ is the set of *base* arcs denoting the communication of UAV u_i to the BS B;

We indicate with $\delta^+(v)$ (resp. $\delta^-(v)$), the outgoing (resp. incoming) arcs of vertex v. Similarly, we indicate with $\delta^+_{r_j}(v)$ (resp. $\delta^-_{r_j}(v)$), the outgoing (resp. incoming) arcs using sub-channel r_j and with $\delta^+_{\text{dt}}(v)$ (resp. $\delta^-_{\text{dt}}(v)$), the outgoing (resp. incoming) arcs related to data packet dt. Fig. 6 depicts an example of multi-graph construction for a small-scale scenario.

4.3. Problem Formulation

Given the multi-graph formulation introduced in the previous Section, the scheduling of data transmission over the cellular UAV-swarm can be modeled as the problem of determining the optimal sequence of arcs (which correspond to networking actions in our modeling) so that the overall probability of successful transmission is maximized. To this purpose, we introduce the following variable:

$$\varphi_a = \begin{cases} 1, & \text{if arc } a \in A \text{ is selected} \\ 0, & \text{otherwise} \end{cases} . \tag{1}$$

Let $\mathcal{W}_a$ denote the probability of successful transmission through arc a, with $a \in \{A_{TR} \cup A_B\}$, i.e. the arc corresponds to a transmission on a U2U or on a U2I link. We model $\mathcal{W}_a$ as follows:

$$\mathcal{W}(a) = \begin{cases} 1 & \text{if } \text{SINR}_a^{\text{SL}}[dBm] > k_2 \\ 0 & \text{if } \text{SINR}_a^{\text{SL}}[dBm] < k_1 \\ (\text{SINR}_a^{\text{SL}}[dBm] - k_1)/(k_2 - k_1) & \text{otherwise} \end{cases} \tag{2}$$

where the constants k_1 and k_2 can be extrapolated from the SINR range in Fig. 4a of Section 3.2. Here, $\text{SINR}_a^{\text{SL}}$ is derived in Section 3.2 and specifies the SINR value at the destination UAV. Its value can be expressed as:

$$\text{SINR}_a^{\text{SL}}[W] = \frac{\varphi_a \cdot \text{rss}(a)}{\sum_{v \in V(t_k)} \sum_{a' \in \delta^+(v)_{r_j}} \varphi_{a'} \cdot \text{rss}(a') + N_0} \tag{3}$$

$$\text{SINR}_a^{\text{SL}}[dBm] = 10 \cdot log_{10}(1000 \cdot \text{SINR}_a^{\text{SL}}[W]) \tag{4}$$

where N_0 refers the received power noise, and $\text{rss}(a)$ is the signal strength received at the destination UAV belonging to arc a. For a single data packet dt, the overall probability can be computed as:

$$\prod_{a \text{ used by dt}} \mathcal{W}(a) \tag{5}$$

It is worth noting that, when the data packet is being delivered over a multi-hop an end-to-end link, the overall packet delivery probability will be constrained by the most unreliable link included in the routing path. Due to the iterative behavior of our optimization model, some cases may result in sub-optimal results of the overall probability induced

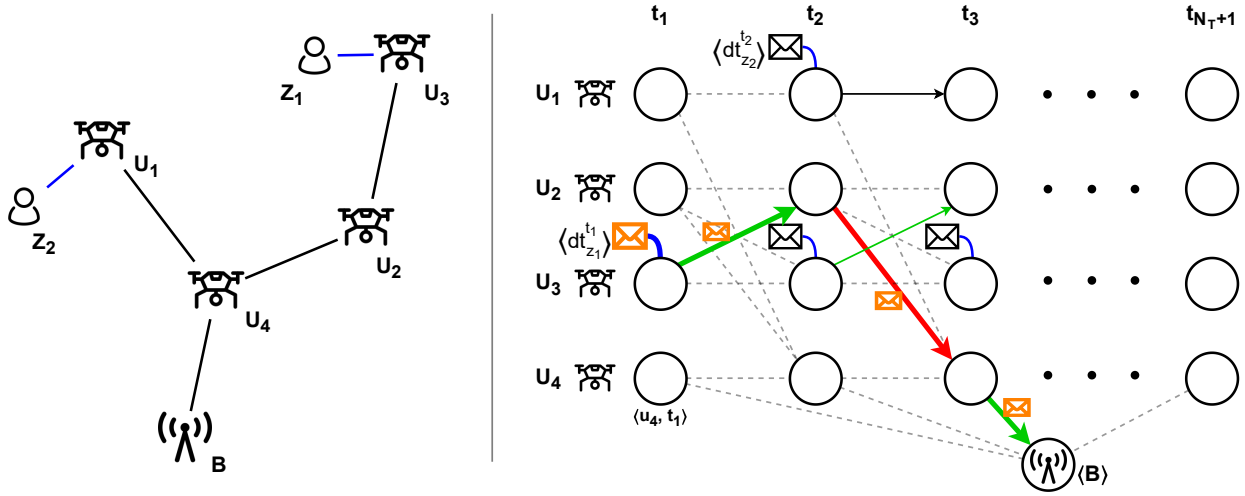

Figure 6: Illustration of the multi-graph construction. On the left, we have the scenario with 4 UAVs (U_1,U_2,U_3,U_4) and 2 PoIs (Z_1,Z_2), while the derived multi-graph is depicted on the right. For ease of drawing, not all the labels are showed. The V_{UAV} vertexes consist of tuples $\langle u_i, t_k \rangle$, the BS node $\langle B \rangle$, and the packets $\langle \mathrm{dt}^{t_k}_{z_j} \rangle$. The colored arrows depict the different channels that are used for transmitting, while the black one shows the buffering of the packet $\langle \mathrm{dt}^{t_2}_{z_2} \rangle$ at UAV u_1. The thick arrows depict the path performed by the packet $\langle \mathrm{dt}^{t_1}_{z_1} \rangle$ (colored in orange).

by the link unreliability experienced in the path. However, we show that, this trade-off does not cause significant performance degradation (*e.g.,* the packer delivery ratio (PDR)) as shown in Fig. 8. During the "positioning" phase, the UAVs form a multi-hop path from PoI towards the base that would ensure communication range constraint. Although the "transmission scheduling" phase follows after "positioning", their estimated locations in the multi-hop chain ensure an end-to-end link being able to deliver the data packet across the chain towards the base. If the SINR experienced through the arc is above certain threshold, the link is active for data transmission and transmit with a probability. We aim at maximizing the probability of successful transmission through a given arc from the channel conditions experienced (*i.e.,* SINR) between transmitter and receiver.

In the scheduling problem, we want to determine the optimal φ_a so that the expected number of packets successfully received by the BS is maximized, considering all the traffic produced in the scenario, i.e.:

$$\underset{\varphi_a}{\operatorname{argmax}} \sum_{\mathrm{dt} \in \mathrm{DT}} \prod_{a \text{ used by dt}} \mathcal{W}(a). \tag{6}$$

Maximizing the value of Equation (6) leads to an highly nonlinear problem. In the following Section, we relax the objective function in order to be able to reformulate the problem and solve it with optimization tools.

5. Proposed Algorithms

This Section presents the proposed algorithms to deploy the cellular UAV-swarm. First, in Section 5.1 we describe a centralized solution to the scheduling problem introduced in Section 4.3. A distributed solution is discussed in Section 5.2. Finally, the UAV positioning scheme is briefly presented in Section 5.3.

5.1. Centralized Solution

In this section, we propose a mathematical model that aims at finding an effective communication schedule by tuning as parameters the path associated to each data packets in the multi-graph presented in Section 4.2, *i.e.,* the φ_a values. More precisely, the optimal solution to the scheduling problem can be obtained by solving the following Multi-Channel Flow Optimization Problem (MCFOP):

$$\min \sum_{a,\in A} b_a \varphi_a + \sum_{a,a' \in A} c_{a,a'} \varphi_a \varphi_{a'} \tag{7}$$

$$\sum_{a \in \delta^+(v)} \varphi_a \leq 1, \qquad \forall v \in V_D \tag{8}$$

$$\sum_{a \in \delta^+_{r_j}(v)} \varphi_a \leq 1, \qquad \forall v \in V_{UAV}, r_j \in \mathcal{R} \tag{9}$$

$$\sum_{a \in \delta^-_{r_j}(v)} \varphi_a \leq 1, \qquad \forall v \in V_{UAV}, r_j \in \mathcal{R} \tag{10}$$

$$\sum_{a \in \delta^+_{\mathrm{dt}}(v)} \varphi_a - \sum_{a \in \delta^-_{\mathrm{dt}}(v)} \varphi_a = 0, \qquad \forall v \in V_{UAV}, r_j \in \mathrm{DT} \tag{11}$$

$$\varphi_a + \varphi_{a'} \leq 1, \qquad \forall v \in V_{UAV}, \; \forall a \in \delta^+(v) \setminus A_{BUF}, \; a' \in \delta^-(v) \setminus A_{BUF} \tag{12}$$

$$\varphi_a \in \{0,1\}, \qquad \forall a \in A \tag{13}$$

The objective function (7) is an approximation of the real objective function max $\sum_{\text{dt}\in\text{DT}} \prod_{a \text{ used by dt}} \mathcal{W}(a)$ and it consists of a linear and a quadratic term. The two terms play two different roles in the search for the optimal solution. The linear term allows to find the shortest routing to the BS. On the other hand, the quadratic term introduces a penalty whether a pairs of arcs a and a' appears together in the solution. In principle, the objective function is written in a generic way that allows to penalize any pair of arcs in the multi-graph G. However, in our implementation, we fixed the values of $b_a = \frac{1}{\mathcal{W}(a)}$, while $c_{a,a'} = 10^2$ if the distance between arcs a and a' is lower than a given threshold D_{interf}, and they have the same time period and same subchannel. In this way the objective function (7) first aims at minimizing the number of times we have a transmission with a potential interference. Secondly, for two solutions with the same number of conflicts, it prefers a solution maximizing the total sum of probabilities of having a successful communication.

Constraint (8) ensures that each data source (*i.e.,* PoI) is associated to at most one UAV. Constraints (9) and (10) ensure that a UAV transmits and receives at most one data packet on the same subchannel during the same subframe period. Constraint (12) ensures that each UAV can only either receive or transmit in a given time t. Finally, Constraint (11) creates a *flow* for the data frames from the source to the BS. In other words, if a node receives a data packet at a given time t, it must either keep it via *buffering* arcs or sent it to another UAV or to the BS via *transmission* or *base* arc.

5.1.1. Complexity of the MCFOP

In this subsection, we prove the complexity of the MCFOP by restriction from the shortest weight-constrained path [34]:

Theorem 1. The MCFOP is NP-hard.

Proof. Given a graph $G = (V, A)$, a set of non-negative length l_a and a non-negative weight w_a for each arc $a \in A$, two specified vertices $s, t \in V$ and positive integers K and W. The Shortest weight-Constrained Path (SCP) searches for a simple path in G from s to t with total weight W or less and total length K or less. The SCP is NP-hard [34]. For a given instance of SCP, let us consider the following restriction of the MCFOP: we fix $N_T = T$, $N_{subc} = 1$, we use G as layout graph, where $\bar{E}_{UAV} = \{\langle s \rangle\}$, t is the base station ($\langle B \rangle = t$) and $\tau_a = t_a$. The linear costs are given by w_a, i.e., $b_a = w_a$ and there are no quadratic costs, i.e., $c_{a,a'} = 0$. With the given transformation, MCFOP compute a SCP of minimal cost with total length less than T, therefore MCFOP is also NP-hard. □

5.2. Dynamic Consensus-Based Bundle Algorithm

The centralized solution assumes a complete knowledge of the UAVs positions and a continuous exchange of control messages between the central BS and the UAV swarm. Given the unfeasibility of such assumptions, and the computational cost of the centralized solution, in this Section we propose a distributed method for channel sharing and transmission scheduling, based on popular auction-based algorithms. Indeed, Consensus-Based Bundle Algorithm (CBBA) [35] is a well-known auction-based method for decentralized task allocation among some agents. CBBA proceeds in repeated iterations of two phases, (1) Bundle construction and (2) Consensus phase. In the first phase, an agent creates task bundle by winning the bid over the other agents. In the second phase, a mutual consensus is applied on the winning bids of agents in order to perform the conflict resolution among the agent-task pairs. The algorithm is shown to converge in real-time and produces a conflict-free assignment of agents to tasks [35]. We model the UAVs as agents and the Transport Blocks (TBs) as tasks that the agents can use to transmit its data. The UAVs must be assigned to different TBs in order to avoid mutual interference.

To this purpose, the task allocation algorithm must produce a conflict-free assignment of N_{task} tasks among N_U UAVs in order to minimize simultaneous transmissions over the shared channels. Let $\mathcal{U}$ be the set of UAVs and $\mathcal{K}$ the set of available tasks. In our modeling, $\mathcal{K} = \{k_1, k_2, \dots, k_{N_{\text{task}}}\}$ represents the pool of TBs that UAVs can reserve to transmit their data. We assume that the time $\mathcal{T}$ is subdivided into superframes $\mathcal{T}^i_{\text{supf}} = \{t_{0+N_{\text{supf}}\cdot i}, t_{1+N_{\text{supf}}\cdot i}, \dots, t_{(N_{\text{supf}}-1)+N_{\text{supf}}\cdot i}\} \subset \mathcal{T}$ of length N_{supf}, where $t^s_k = t_{k+N_{\text{supf}}\cdot i}$ that represents the k-th time slot inside every superframe. The task $k_j \in \mathcal{K}$ is hence defined as a pair $\langle t^s_k, r_y \rangle$, with $r_y \in \mathcal{R} \setminus \{r_0\}$ being an available subchannel (see Figure 7). The number of tasks is given by: $N_{\text{task}} = N_{\text{supf}} \cdot N_{\text{subc}}$. The CBBA algorithm envisages the possibility for each agent to perform L_t tasks during the algorithm execution. Initially, we assume this value to be homogeneous among the UAVs and equal to the packet generation rate from the PoIs (N_g). How to remove the assumption is discussed later in this Section.

During the first phase, the CBBA algorithm keeps track of the following lists: (*i*) the winning bid list $\mathbf{y}_i$ of length N_{task} containing the bid of the winning agent; (*ii*) the winning UAV list $\mathbf{z}_i$ of length N_{task} containing the the winning UAV for each specific TB in the resource pool; (*iii*) and a bundle $\mathbf{b}_i$ that contains the list of the TBs obtained by UAV i. Let c_{ij} be the score function, defining the reward for UAV i using the TB k_j for the transmission. We define the score function as follow:

$$c_{ij} = \begin{cases} 1 & \text{if } \text{rss}_j \leq \text{rss}_{\min} \\ \frac{1}{1+(\text{rss}_j - \text{rss}_{\min})} & \text{otherwise} \end{cases} \tag{14}$$

where rss_j is the estimation of the received signal strength detected at the TB of task k_j in the previous superframes, while $\text{rss}_{\min}$ is a system threshold on the rss under which the sub-channel is detected as idle. The aim of the distributed assignment algorithm is to maximize the value of $\sum_{u_i \in \mathcal{U}} \sum_{k_j \in \mathcal{K}} c_{ij} \cdot \text{x}_{ij}$, i.e. to minimize the simultaneous transmissions of different UAVs on the same TB. Here, x_{ij} is 1 if UAV i uses the TB k_j, and 0 otherwise. Algorithm 1 shows the first phase of the bundle construction. The bundle construction is executed at each t^s_0, i.e. at the beginning of

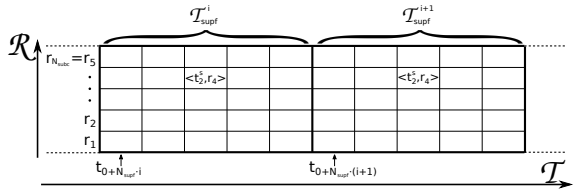

Figure 7: Tasks definition: in this example, two consecutive task pools are depicted, $\mathcal{T}^{i}_{\text{supf}}$ and $\mathcal{T}^{i+1}_{\text{supf}}$, where $N_{\text{subc}} = 5$ and $N_{\text{supf}} = 5$.

each superframe.

Algorithm 1: Bundle Construction

Input: $\mathbf{y}_i, \mathbf{z}_i, \mathbf{b}_i$

1 **while** $|\boldsymbol{b}_i| < L_t$ **do**
2 $\quad h_{ij} \leftarrow \mathbb{I}(c_{ij} > y_{ij}) \quad \forall k_j \in \mathcal{K}$
3 $\quad J_i = \text{argmax}_j(c_{ij} \cdot h_{ij})$
4 $\quad \mathbf{b}_i \leftarrow \mathbf{b}_i \cup \{k_j\}$
5 $\quad y_{i,j} \leftarrow c_{i,J_i}$
6 $\quad z_{i,j} \leftarrow i$
7 **end**

In Algorithm 1, we assume that at time t_0 the elements in the sets $\mathbf{y}_i$ and $\mathbf{z}_i$ are initialized to 0, and $\mathbf{b}_i$ to $\emptyset$, $\forall u_i \in \mathcal{U}$. The algorithm starts with checking the $\mathbf{b}_i$ set that must contain L_t elements, i.e. the requested packets to transmit (line 1). Inside the while loop, the algorithm chooses the best task whose score function is greater then the winning bid (lines 2 and 3). Here, the $\mathbb{I}$ function returns 1 if the argument is true, 0 otherwise. Finally, the bundle $\mathbf{b}_i$ is updated with the winning task, and consequently the sets $\mathbf{y}_i$ and $\mathbf{z}_i$ (lines 4 - 6).

Each UAV broadcasts a beacon message every T_{beacon} seconds, in order to exchange control information used for the consensus phase performing conflict resolution. This message contains the winning bids list $\mathbf{y}_i$, the winning agents list $\mathbf{z}_i$, and the list $\mathbf{s}_i$, with $|\mathbf{s}_i| = N_U$, indicating the timestamp referring the last received beacon from the other UAVs. At every beacon reception from UAV u_j, the UAV i activates the conflict resolution phase that consists in the execution of a set of check rules listed in [35] for every element in $\mathbf{z}_j$. Each rule serves to update the conflicts on the task assignment, by allocating the tasks to the UAVs with the greatest bid.

The Algorithm 1 described so far considers a static number of tasks for each UAV u_i, given by the value of L_t. However, the need of transmission opportunities within cellular UAV swarms may change dynamically as a consequence of varying traffic loads, new mission requirements, interference effects, etc. For this reason, let L^i_t be the number of tasks for each agent $u_i \in \mathcal{U}$ and at each time slot t_k. In the following, we introduce a variant of the CBBA algorithm, named *Dynamic-CBBA* (D-CBBA), that takes into account the presence of $L^i_t(t_k)$ terms for each UAV/time slot. The algorithm works similar to the legacy CBBA algorithm and is composed of a sequence of a bundle construction phases followed by a conflict resolution phase. However, differently from the legacy CBBA algorithm, we need to add a decision rule to the decision table defined in [35], in order to deal with the variability of assigned tasks. This rule is defined in Table 4.

Table 4
D-CBBA extra decision rule

Agent i thinks $z_{i,j}(t_k)$ is	Agent i thinks $z_{i,j}(t_{k+1})$ is	Action
i	i	$L^i_t(t_{k+1}) < L^i_t(t_k)$ ⇓ ResetWorst

The action "ResetWorst" resets both the winning bid and the agent, i.e. $y_{i,j} = 0$ and $z_{i,j} = 0$ of the worst task belonging to the winning bundle $\mathbf{b}_i$ at time t_k, i.e. k_w with $w = \text{argmin}_j\, c_{ij}$ where $x_{iw} = 1$. This new rule allows to release the resource when it is no longer needed by the UAV. For the D-CBBA algorithm, we define the number of tasks to assign to the UAV u_i as $L^i_t(t_k) = \text{queue}_i(t_k) + \text{hist}_i(t_k)$, where $\text{queue}_i(t_k)$ indicates the packet queue size of UAV u_i at time slot t_k, while $\text{hist}_i(t_k)$ is the number of packets received during the last N_{supf} time slots. In this way, the UAV will be able to obtain enough TBs to transmit the packets from the transmission queue plus an estimation of packets that the UAV will receive during the next superframe. It is worth mentioning that the value of $L^i_t(t_k)$ must be less or equal than the number of available tasks N_{task}.

5.2.1. Computational complexity

The computational complexity of the bundle construction phase, i.e. Algorithm 1, is defined by the main loop of line 1, that is executed $\mathcal{O}(L_t)$ times. Inside the loop, the research of the best task is $\mathcal{O}(N_{\text{task}})$ due to the linear research of the argmax value (line 3). Given that the maximum value that L_t can get in our D-CBBA algorithm is N_{task}, the total computational complexity of the bundle construction phase is $\mathcal{O}(N^2_{\text{task}})$.

The second phase, i.e. the conflict resolution, is activated

Table 5
Simulation Parameters

Component	Model
N_U	10
M	10 km
N_Z	4
N_{supf}	20
N_{subc}	3
N_g	400
D_{comm}	1000 m
D_{interf}	1200 m
T_{beacon}	0.2 s
rss_{min}	-105 dBm
BUF_{max}	500

at each UAV u_i upon reception of a beacon message form UAV u_j. During this phase, the elements of $\mathbf{z}_j$ are visited and, for each element, the table check is executed. We recall that $|\mathbf{z}_j| = N_{\text{task}}$. The rules defined in CBBA [35] are executed in constant time, $\mathcal{O}(1)$, while the action "ResetWorst" defined in Table 4 is $\mathcal{O}(N_{\text{task}})$ due to its argmin search over all the possible tasks. In conclusion, also the the second phase has a computational complexity of $\mathcal{O}(N_{\text{task}}^2)$.

5.3. Positioning Algorithm

We assume that the positioning algorithm is computed in a centralized way by the BS before the starting of the mission. The goal is to maximize the the coverage of PoIs from the UAVs. To this aim, we assume that a Minimum Spanning Tree (MST) algorithm is used, where the vertexes are the PoIs and the BS, while the weights of the arcs are defined as the Euclidean distance between the vertexes. The Prim's algorithm is executed to compute the tree. Finally, the UAVs are placed on the edges at a maximum distance of D_{comm} in order to ensure that the swarm is fully connected.

6. Experimental Setup and Performance Results

The simulation setup considers a swarm of cellular-connected UAVs performing video monitoring tasks of N_Z target regions. The monitoring regions are placed randomly in a map scenario of size $M \times M$ square meters. There are N_U UAVs statically placed using the MST algorithm with an inter-UAV distance of at most D_{comm} meters. The BS is placed at the center of the scenario. The simulation parameters are reported in Table 5. The UAVs that are positioned at the PoIs represent the end nodes of the MST and are in charge of generating sensing data with a rate of N_g packets per second.

We compare these scheduling algorithms in the performance evaluation:

- *Centralized Solution with Limited Interference*: This is the algorithm presented in Section 5.1, by considering an interference radius equal to D_{interf} meters. It is abbreviated as Centralized (Lim. Int.) in the plots.
- *Centralized Solution*: this is the above mentioned algorithm after removing the assumption on the limited interference radius.
- *CBBA*: This is the state-of-the-art distributed algorithm with the application described in Section 5.2 and a static number of tasks. Specifically, we set $L_t = N_g$.
- *D-CBBA*: This is our extension of the *CBBA* algorithm with varying number of tasks for UAVs, described in Section 5.2.
- *Greedy Algorithm*: This is a basic scheme where each UAV randomly selects the TBs for data transmission, without any explicit cooperation with other peers. It is used here as baseline for distributed resource allocation.

The centralized solution is evaluated with mathematical optimization framework by solving the optimization problem stated in Equation 7 and Equations 8-12. This model is implemented in C++ using IBM ILOG CPLEX 12.8.0 [36] as MILP solver. All experiments are executed on a single core of an Intel Xeon E5-4620 at 2.2GHz with 4GB of available memory. The distributed solution is evaluated via extensive simulations. The Packet Delivery Ratio (PDR) is used as key performance metric.

Figures 8a and 8b depict the PDR with respect to the varying rate of packet generation (N_g) and number of sub-channels (N_{subc}), respectively. As expected, the PDR is negatively correlated with the data generation rate and positively correlated with the number of available sub-channels. When increasing the packet generation ratio, in fact, the network becomes more and more congested; as a result, it becomes challenging to allocate idle TBs to only one UAV. Vice versa, the interference decreases when expanding the pools of available sub-channels from which the UAVs can pick up the TBs.

From these Figures, we can observe the difference between the two centralized solutions and more specifically the impact of the approximation introduced in Section 5.1 to make the problem tractable. The centralized solution with limited interference adds the assumption of a limited interference radius, equal to D_{interf} meters; it is easy to notice that the assumption produces a PDR equal to 98%. If we keep the same transmission scheduling but remove the assumption of limited interference radius, we can notice an additional loss of around 2% in the performance. This is mainly due to packet collisions occurring on links covering long distances and hence with reduced SINR values.

Moving the analysis to the distributed solutions, we can appreciate the differences between the D-CBBA, the CBBA and the Greedy algorithm. The Greedy algorithm perform worse than the other schemes with a PDR value close to 0.8 with $N_g = 500$ and $N_{\text{subc}} = 3$. This is due to the lack of coordination among the UAVs that select the RBs in a pure random basis. Differently, both CBBA and the D-CBBA schemes introduce coordination among the UAVs; in particular, the D-CBBA self-adapts to the network requests, thus it reserves only the resources needed at each superframe. We can notice that D-CBBA performs similar to the centralized solution, where the transmissions are coordinated by the central BS. The choice of the score function c_{ij} (Equation 14) has a fundamental impact on the performance of CBBA algorithms. In this case, UAVs that are close to each other are able to avoid the selection of the same TBs for the transmission. However, when the network becomes crowded, due to the increasing traffic load or the small number of available channels, the CBBA algorithm is able to avoid interference between close UAVs, hence reducing the impact on the SINR on the receiver UAVs. Furthermore, the dynamic choice of the L_t^i value in the D-CBBA algorithm allows a more adaptive scheme, where the UAVs reserve only the exact amount of resources needed.

Figure 9a confirms the analysis described so far. Indeed,

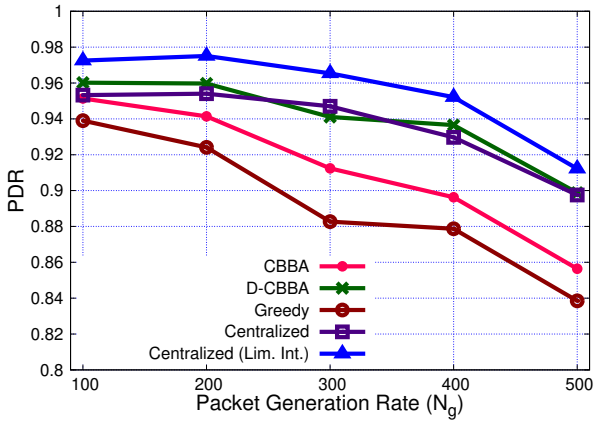

(a) PDR varying with rate of packet generation (N_g)

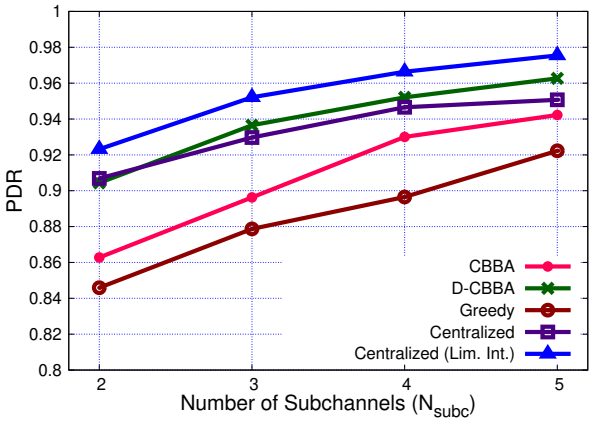

(b) PDR varying with number of subchannels (N_{subc})

Figure 8: Variability of PDR

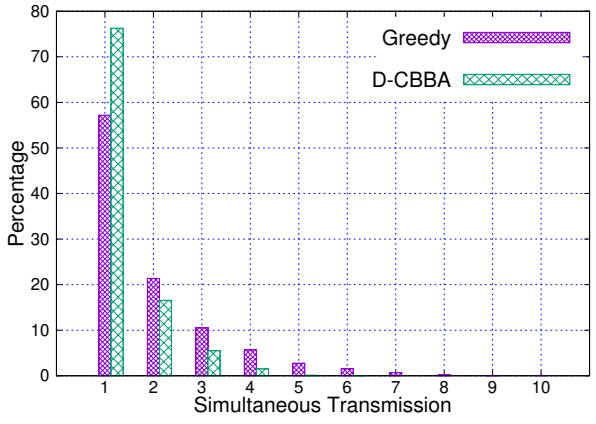

(a)

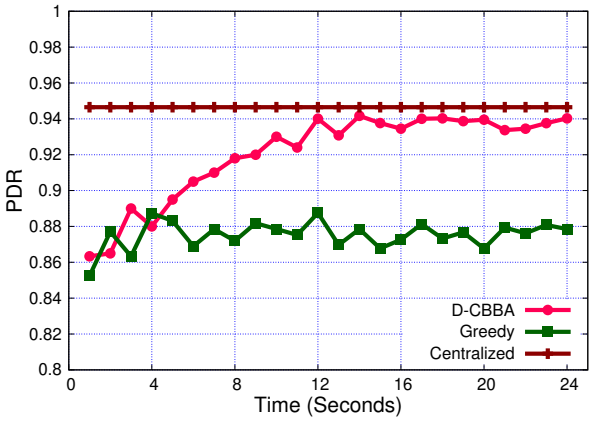

(b)

Figure 9: (a) Percentage of simultaneous transmissions for Greedy and D-CBBA, (b) Comparison of the algorithm convergence time.

the Figure shows the number of simultaneous transmissions and hence it reflects the ability of the algorithms in avoiding potential concurrent access to the shared resources. The D-CBBA algorithm is able to successfully complete more than 75% of data transmissions without generating interference, while the Greedy algorithm can barely reach 60%. Fig. 9b evaluates the convergence time of the D-CBBA algorithm. The system reaches a steady state nearly at 12 *sec* where the PDR stabilizes to a value around 0.94. The algorithm, in fact, exchanges control messages every T_{beacon} seconds in order to reach the consensus on the data transmission scheduling decisions. On the contrary, the Greedy algorithm does not exchange messages and behaves in the same manner for the entire duration of the simulation.

Finally, Figures 10a and 10b investigate the impact of the superframe size N_{supf} on the PDR and end-to-end delay. The two algorithms behaves similarly, with an increasing trend of the end-to-end delay. Indeed, for larger superframe size, there may be unused TBs which introduce additional delays in the packet transmission. On the other side, the PDR is not affected by the variation of the superframe size. Again, we can appreciate the ability of the D-CBBA algorithm to adapt to the network conditions when choosing the number of requested tasks, i.e. the number of transmissions inside each superframe. Such value depends, indeed, on the estimated number of packets that should be sent during the next superframe, and therefore, the scheme adapts to its size.

7. Conclusions and Future Outlook

In this work, the problem of cooperative and communication-aware UAV positioning and channel scheduling is investigated in order to carry out the data transmission from a set of target points towards cellular BS. The range of UAV radios are finite and hence, they tend to fly beyond the BS coverage in a typical mission. Considering the limited coverage, we studied a cooperative, multi-hop sidelink-assisted design of C-U2X communication model that optimizes the scheduling decisions of data transmission employing sidelink sub-channels. The model is validated using both centralized and distributed algorithms. The formulated problem is solved in centralized

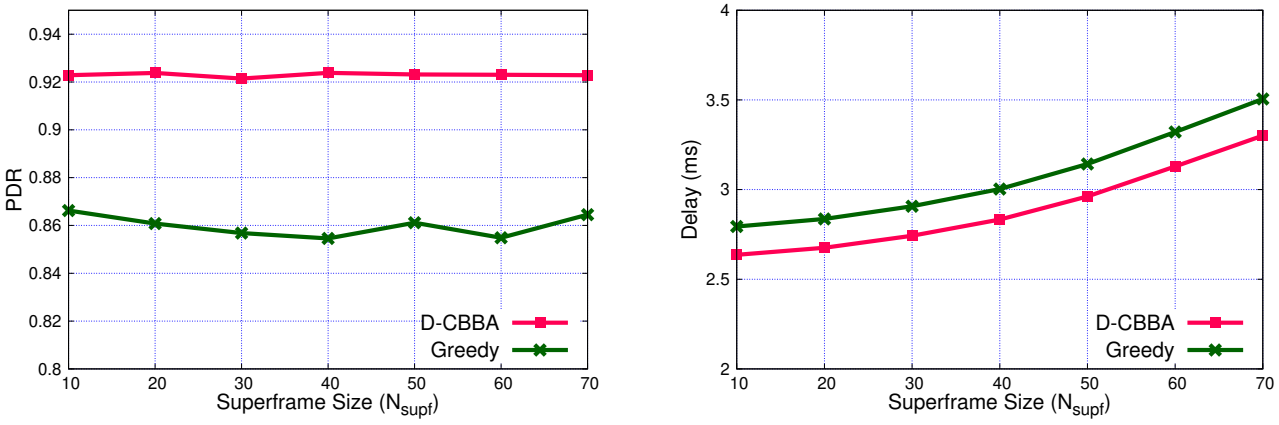

(a) PDR Variation

(b) Delay Variation

Figure 10: PDR and Delay varying with superframe size (N_{supf}).

manner by mathematical optimization framework. A distributed auction-class of algorithms, D-CBBA is proposed to generate efficient sub-channel scheduling decision for maximizing data transmission from PoIs to central BS. Our experimental assessment demonstrates that the distributed algorithm potentially enhances the cellular infrastructure coverage via multi-hop communications over the 5G sidelink. In the future, we aim at building a real-world working prototype of the cellular-connected UAV swarm based on sidelink and study its performance characteristics with realistic flight plans. In addition, we plan to expand the optimization model in order to jointly consider the phases of UAV positioning and data scheduling.

References

[1] Y. Zeng, Q. Wu, R. Zhang, Accessing from the sky: A tutorial on UAV communications for 5G and beyond, Proceedings of the IEEE 107 (12) (2019) 2327–2375.

[2] M. Mozaffari, et al., A Tutorial on UAVs for Wireless Networks: Applications, Challenges, and Open Problems, IEEE communications surveys & tutorials 21 (3) (2019) 2334–2360.

[3] D. Mishra, N. R. Zema, E. Natalizio, A High-End IoT Devices Framework to Foster Beyond-Connectivity Capabilities in 5G/B5G Architecture, IEEE Communications Magazine 59 (1) (2021) 55–61.

[4] D. Mishra, E. Natalizio, A Survey on Cellular-connected UAVs: Design Challenges, Enabling 5G/B5G Innovations, and Experimental Advancements, Computer Networks 182 (2020) 107451. doi:https://doi.org/10.1016/j.comnet.2020.107451.
URL http://www.sciencedirect.com/science/article/pii/S1389128620311324

[5] Y. Zeng, J. Lyu, R. Zhang, Cellular-connected UAV: Potential, challenges, and promising technologies, IEEE Wireless Communications 26 (1) (2018) 120–127.

[6] E. Yanmaz, et al., Communication and Coordination for Drone Networks, Ad hoc networks (2017) 79–91.

[7] G. Skorobogatov, et al., Multiple UAV systems: A Survey, Unmanned Systems 8 (2) (2020) 149–169.

[8] M. Campion, P. Ranganathan, S. Faruque, UAV swarm communication and control architectures: a review, Journal of Unmanned Vehicle Systems 7 (2) (2018) 93–106.

[9] X. Chen, J. Tang, S. Lao, Review of Unmanned Aerial Vehicle Swarm Communication Architectures and Routing Protocols, Applied Sciences 10 (10) (2020) 3661.

[10] P. Chandhar, et al., Massive MIMO for Communications With Drone Swarms, IEEE Transactions on Wireless Communications 17 (3) (2017) 1604–1629.

[11] A. Garcia-Rodriguez, et al., The Essential Guide to Realizing 5G-Connected UAVs with Massive MIMO, IEEE Communications Magazine (2019).

[12] A. Asadi, Q. Wang, V. Mancuso, A Survey on Device-to-Device Communication in Cellular Networks, IEEE Communications Surveys Tutorials 16 (4) (2014) 1801–1819. doi:10.1109/COMST.2014.2319555.

[13] F. Jameel, Z. Hamid, F. Jabeen, S. Zeadally, M. A. Javed, A Survey of Device-to-Device Communications: Research Issues and Challenges, IEEE Communications Surveys Tutorials 20 (3) (2018) 2133–2168. doi:10.1109/COMST.2018.2828120.

[14] M. Gonzalez-Martín, M. Sepulcre, R. Molina-Masegosa, J. Gozalvez, Analytical models of the performance of c-v2x mode 4 vehicular communications, IEEE Transactions on Vehicular Technology 68 (2) (2019) 1155–1166. doi:10.1109/TVT.2018.2888704.

[15] N. Bonjorn, et al., Enhanced 5G V2X Services using Sidelink Device-to-Device Communications, 2018 17th annual mediterranean ad hoc networking workshop (Med-Hoc-Net) (2018) 1–7.

[16] R. Molina-Masegosa, J. Gozalvez, LTE-V for sidelink 5G V2X vehicular communications: A new 5G technology for short-range vehicle-to-everything communications, IEEE Vehicular Technology Magazine 12 (4) (2017) 30–39.

[17] S.-Y. Lien, et al., 3GPP NR Sidelink Transmissions Toward 5G V2X, IEEE Access 8 (2020) 35368–35382.

[18] K. Ganesan, et al., NR Sidelink Design Overview for Advanced V2X Service, IEEE Internet of Things Magazine 3 (1) (2020) 26–30.

[19] D. Mishra, A. Vegni, V. Loscri, E. Natalizio, Drone Networking in 6G Era-A Technology Overview, IEEE Communications Standards Magazine (2022).

[20] S. Xiaoqin, M. Juanjuan, L. Lei, Z. Tianchen, Maximum-throughput sidelink resource allocation for nr-v2x networks with the energy-efficient csi transmission, IEEE Access 8 (2020) 73164–73172.

[21] A. Mansouri, V. Martinez, J. Härri, A first investigation of congestion control for lte-v2x mode 4, in: 2019 15th Annual Conference on Wireless On-demand Network Systems and Services (WONS), 2019, pp. 56–63.

[22] V. P. Karamchedu, A Path from Device-to-Device to UAV-to-UAV Communications, in: 2020 IEEE 92nd Vehicular Technology Conference (VTC2020-Fall), 2020, pp. 1–5. doi:10.1109/VTC2020-Fall49728.2020.9348841.

[23] D. Mishra, A. Trotta, M. Di Felice, E. Natalizio, Performance Analysis of Multi-hop Communication based on 5G Sidelink for Cooperative UAV Swarms, in: 2021 IEEE International Mediterranean Conference on Communications and Networking (MeditCom), 2021, pp.

395–400. doi:10.1109/MeditCom49071.2021.9647449.

[24] M. M. Azari, et al., Cellular UAV-to-UAV Communications, 30th IEEE PIMRC (2019) 1–7.

[25] M. M. Azari, et al., UAV-to-UAV Communications in Cellular Networks, IEEE Transactions on Wireless Communications (2020).

[26] S. Zhang, H. Zhang, B. Di, L. Song, Cellular uav-to-x communications: Design and optimization for multi-uav networks, IEEE Transactions on Wireless Communications 18 (2) (2019) 1346–1359.

[27] M. Li, S. Salinas, P. Li, X. Huang, Y. Fang, S. Glisic, Optimal Scheduling for Multi-Radio Multi-Channel Multi-Hop Cognitive Cellular Networks, IEEE Transactions on Mobile Computing 14 (1) (2015) 139–154. doi:10.1109/TMC.2014.2314107.

[28] L. Song, M. Tao, Y. Xu, Exploiting hop diversity with frequency sharing in multi-hop ofdm networks, IEEE Communications Letters 13 (12) (2009) 908–910. doi:10.1109/LCOMM.2009.12.091902.

[29] Q. N. Tran, et al., Downlink Resource Allocation Maximized Video Delivery Capacity over Multi-hop Multi-path in Dense D2D 5G Networks, in: 2020 4th International Conference on Recent Advances in Signal Processing, Telecommunications Computing (SigTelCom), 2020, pp. 72–76. doi:10.1109/SigTelCom49868.2020.9199027.

[30] Zhifeng He, et al., Link scheduling and channel assignment with a graph spectral clustering approach, in: MILCOM 2016 - 2016 IEEE Military Communications Conference, 2016, pp. 73–78. doi:10.1109/MILCOM.2016.7795304.

[31] M. M. Azari, F. Rosas, S. Pollin, Cellular connectivity for UAVs: Network modeling, performance analysis, and design guidelines, IEEE Transactions on Wireless Communications 18 (7) (2019) 3366–3381.

[32] H. ElSawy, A. Sultan-Salem, M.-S. Alouini, M. Z. Win, Modeling and analysis of cellular networks using stochastic geometry: A tutorial, IEEE Communications Surveys & Tutorials 19 (1) (2016) 167–203.

[33] A. Trotta, M. Di Felice, L. Bedogni, L. Bononi, F. Panzieri, Connectivity recovery in post-disaster scenarios through cognitive radio swarms, Computer Networks 91 (2015) 68 – 89.

[34] M. R. Garey, D. S. Johnson, Computers and intractability, A Guide to the (1979).

[35] H. Choi, et al., Consensus-based decentralized auctions for robust task allocation, IEEE Transactions on Robotics 25 (4) (2009) 912–926.

[36] IBM, 2013. IBM ILOG CPLEX 12.8 User Manual. IBM Corp. URL http://public.dhe.ibm.com/software/products/Decision_Optimization/docs/pdf/usrcplex.pdf.